

Investigation of Planar Antennas for Submillimeter Receivers

ULRICH KOTTHAUS AND BERND VOWINKEL, MEMBER, IEEE

Abstract — A frequency-scaled model of a tapered slot antenna has been investigated. The antenna consists of a dielectric substrate which serves as a carrier for a tapered slotline. The width and the shape of the slotline and the dimensions of the substrate (including the value of the permittivity) have been varied to investigate the radiation patterns.

The result is a planar antenna with a symmetrical beam in the *E* and *H* planes and a beam efficiency of almost 50 percent. The substrate thickness is the most important limiting factor for scaling the model to submillimeter frequencies. Taking away parts of the dielectric substrate in the front area of the antenna allows a relatively large substrate thickness.

The variations of the half-power beam width versus slot parameters, versus the dielectric thickness of the substrate, and versus the length and the width of the substrate are presented. In addition the beam efficiency has been measured for various frequencies, and the radiation pattern has been calculated for comparison.

I. INTRODUCTION

MOST MILLIMETER and submillimeter receivers work with horn antennas as receiving elements. They have historically been the most common microwave antenna feed types. The horns are almost always used in waveguide systems, where the radiation is guided to mixers and amplifiers by hollow waveguides. Although the attenuation of fundamental-mode waveguides at higher frequencies, especially at submillimeter frequencies, is extremely high, horn antennas and fundamental-mode waveguides have been produced for these wavelengths. At higher frequencies, however, the dimensions of horns and waveguides become extremely small, so that it takes much effort to fabricate those components with sufficient precision. An interesting alternative is the use of planar antennas.

The class of planar antennas can be subdivided into two main groups: broadside and end-fire antennas. A broadside antenna radiates in a direction perpendicular to the plane of the antenna. Well-known examples are the bow-tie [8] and the logarithmic-periodic spiral antenna [13]. The end-fire planar antennas have radiation patterns with the maximum of radiation in the plane of the antenna. Examples of this type are the V antenna [7], [9], the linear tapered slot antenna [1], and the Vivaldi antenna, first developed by Gibson in 1979 [2].

Manuscript received January 20, 1988; revised July 14, 1988. This work was supported by the Deutsche Forschungsgemeinschaft (DFG), Sonderforschungsbereich 301.

The authors are with the 1. Physikalisches Institut, Universität zu Köln, Zülpicherstr. 77, D-5000 Köln 41, West Germany.

IEEE Log Number 8824998.

We have investigated various planar tapered slot antennas in a frequency-scaled version at about 10 GHz. The aim was to develop a planar antenna with a symmetrical beam pattern in the *E* and *H* planes. The side lobe level should be 15 dB below maximum. A difficult requirement is to ensure that the antenna can be fabricated after scaling all dimensions to submillimeter frequencies. The most critical value is the thickness of the substrate. The beam pattern will no longer be symmetrical and the level of the side lobes will increase dramatically if the substrate thickness is too large. On the other hand the thickness of the substrate should not be too small because of the problems encountered in fabricating the antenna at the final dimensions.

An important characteristic of an antenna is its main beam efficiency. The open structure of the planar antennas does not allow main beam efficiencies as high as those of horn antennas. This disadvantage is outweighed by the interesting possibility of producing closely packed arrays of planar antennas and using them as a multiple-beam system. For a passive imaging radiometer, a system with *N* individual beams yields an *N*-fold increase in mapping speed; alternatively the array can increase the power sensitivity of a receiver by a factor of \sqrt{N} for a given mapping speed.

Two other advantages of the planar antenna are that it is easy to integrate the feeds with mixer or amplifier devices on the same substrate that carries the antenna structure, and it is possible to put a large number of planar antennas on the same substrate. They can be produced using photolithographic techniques, reducing the additional costs for a multiple-beam system.

II. INVESTIGATION OF THE PLANAR ANTENNA IN A FREQUENCY-SCALED VERSION

A. Beam Patterns and Shapes of the Antenna

Fig. 1(a) shows the model antenna for a frequency of 8.5 GHz. In the front area of the antenna a part of the dielectric substrate has been removed to improve the antenna characteristics. The substrate is a dielectric material consisting of a mixture of Teflon and alumina; its permittivity is 10.5, which is close to the permittivity of silicon ($\epsilon_r = 11.3$). One side of the substrate is covered with a layer of copper with a thickness of 35 μm . The substrate of the final antenna at submillimeter frequencies could be

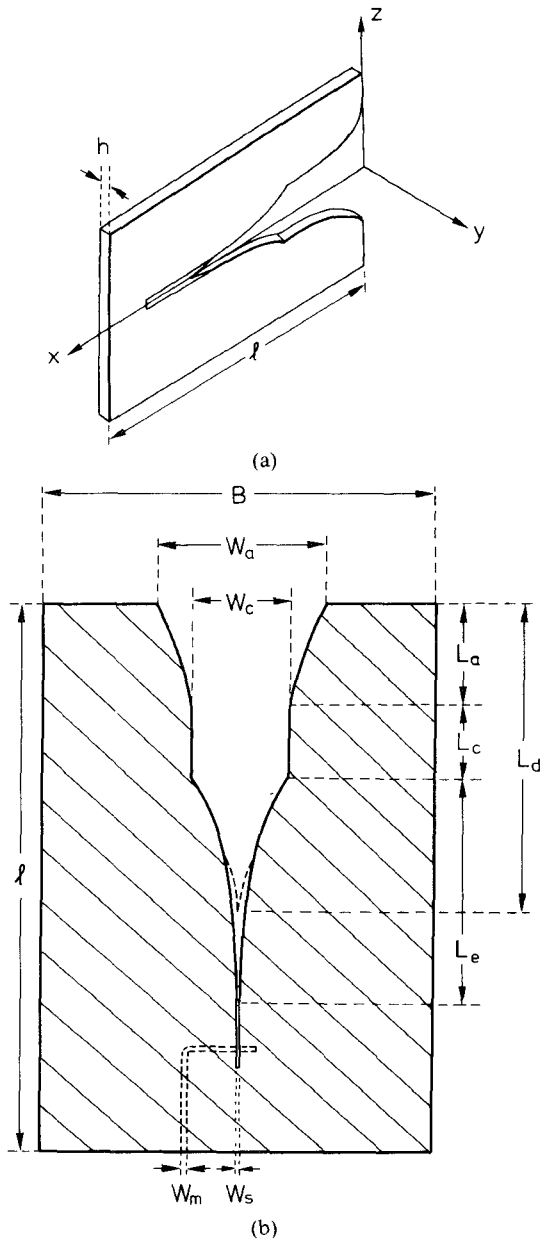


Fig. 1. (a) Planar slot antenna; perspective sketch with coordinate system. (b) Top view of the antenna with slot-to-microstrip transition and important dimensions (given in the text), substrate permittivity: $\epsilon_r = 10.5$.

silicon, which is available with the required small thickness. Another advantage of silicon is that it can be etched, so it will be possible to take away a certain amount of the substrate even at the final dimensions, which will be smaller than the dimensions of the model by a factor of 30 to 70.

A top view of the antenna is shown in Fig. 1(b). The length l is 110 mm; the width B of the antenna is 75 mm. The dielectric substrate serves as a carrier for the antenna structure, which is a tapered slotline. The front taper results in a bandwidth higher than that which an antenna with a constant slot would have and transforms the free-space impedance (377 Ω) to the impedance of the slotline. The width W_a of the slotline at the front end of the antenna is 35 mm. The exponentially tapered section ends

in a constant-width slotline ($W_c = 19$ mm, $L_c = 15$ mm) with a length L_a of 25 mm. The exponential taper of length $L_e = 50$ mm transforms the constant-width slotline to a slotline of width $W_s = 0.9$ mm.

The received power is detected by a coaxial detector via a slotline-to-microstrip transition, as can be seen in Fig. 1(b). This transition uses a cross junction. The slotline etched on one side of the substrate is crossed at a right angle by a microstrip conductor on the opposite side. The slot and the microstrip line each extend about one quarter of a wavelength beyond their intersection. In [6] Knorr presents an equivalent circuit of a slotline-to-microstrip transition and gives some conditions which have to be fulfilled for a perfect match. The main result is that the optimal impedance of the microstrip line can be calculated from the parameters of the slotline. At a frequency of 8.5 GHz, the microstrip impedance should be 70Ω for a slotline impedance of 93Ω . For this transition, a *VSWR* value less than 1.6 has been obtained from 7.5 to 9 GHz. The lowest value reached at 8.5 GHz is 1.2.

Janaswamy and Schaubert [15] have developed a method which allows the calculation of the beam patterns of tapered slot antennas. This analysis consists of two steps. In the first step, the tangential component of the electric field distribution (z direction, see Fig. 1(a)) in the tapered slot is calculated. After Janaswamy *et al.*, the x -directed slot field contributes only to the cross-polarized radiation in either principal plane, and is therefore not considered in the calculations. The presence of the dielectric is accounted for in this first step, but is ignored in the second one, where the far fields radiated by the slot fields are obtained. The continuous taper of the slotline is approximated by a number of sections of uniform width connected end to end. The characteristic impedance, the slot wavelength, the slot electric field, and the radiated far-zone field are calculated for each of these uniform sections. The radiation of the antenna can then be obtained by adding up the contributions from all sections of the approximated slotline. So it is possible to assume a dielectric constant which is not the same for all sections.

The model is ideally valid for an antenna with an infinite extent in the z direction, but Janaswamy *et al.* [15] also found an acceptable agreement with measurements for antennas with lateral dimensions of 3 wavelengths.

We calculated the beam patterns of the tapered slot antenna shown in Fig. 1 with and without parts of the substrate removed.

In Fig. 2 the calculated and measured beam patterns of the antenna in the E plane with no substrate removed are shown. The E plane is defined as the $x-z$ plane (see Fig. 1(a)). For the calculations the tapered slotline was approximated by six sections of uniform width. After Janaswamy *et al.* [15] a good agreement with experiment is obtained for relatively thin substrates ($h/\lambda_0 \approx 0.01$) with permittivities of 2 or 3. For thicker substrates, especially for those with high permittivities, a poorer agreement with experiment can be seen. In addition they found that the calculated slot wavelengths were higher than the measured value

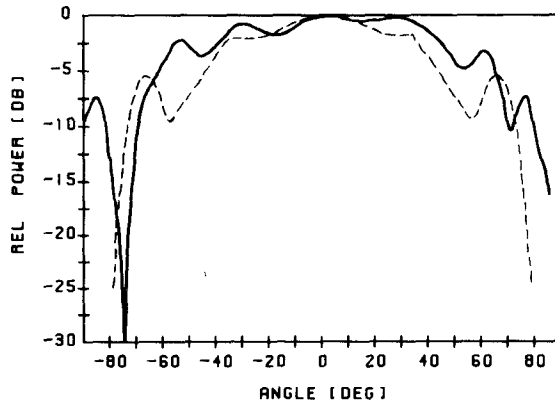


Fig. 2. *E*-plane beam patterns of the slot antenna at 8.5 GHz; substrate thickness is 1.27 mm, permittivity $\epsilon_r = 10.5$, no substrate removed, --- calculated pattern, — measured pattern.

for a particular substrate. This can have dramatic effects on the pattern beam widths and in the side lobe level, especially in the *H* plane. The width *B* of the antenna, which is considered to be infinite in these calculations, has a more pronounced effect on the *E*-plane pattern than on the *H*-plane pattern.

The slotline field components are not confined to the substrate alone. They extend into the air regions above the slot and below the substrate. Therefore, the energy is distributed between the substrate and the air regions. Consequently, the effective dielectric constant is less than the substrate permittivity ϵ_r . Thus, removing parts of the substrate has an additional effect on the effective permittivity of the slotline. As a consequence, the slot wavelength is different from that with no substrate removed. The slot wavelength has a more pronounced effect in the *H*-plane pattern than in the *E*-plane pattern. This is because the *H*-plane pattern depends on the slot wavelength (i.e., on the phase velocity of the traveling wave) and on the antenna length. The *E*-plane pattern is much more sensitive to a change of the slot taper shape.

We calculated the beam patterns of the antenna, although no exact model was available for calculating the effective dielectric constant for parts of the substrate being removed. The tapered slotline was approximated by ten steps, and the effective permittivity was estimated to be 2.2 in the front area of the tapered slotline. From a distance $L_d = 63$ mm measured from the aperture end of the antenna (see Fig. 1) up to the end of the slotline the permittivity is 10.5. In the region where the substrate is not completely removed, the permittivity is assumed to increase from 2.2 to a value of 10.5. In Fig. 3 the calculated and measured radiation patterns in the *E* and *H* planes are shown for the planar antenna as in Fig. 1. The *E* plane is defined as in the $x-z$ plane, the *H* plane as the $x-y$ plane, as indicated in Fig. 1(a). These measured patterns were obtained with optimized dimensions of the tapered slotline and an optimized shape of the missing substrate, as can be seen in Fig. 1(b). The beam is fairly symmetric in the principal planes. The half-power beamwidth is 50° ; depending on the application, it may be

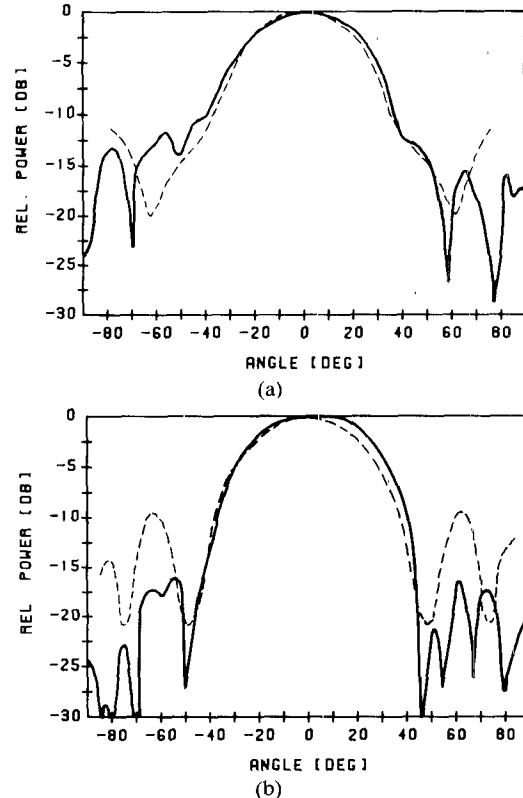


Fig. 3. (a) *E*-plane beam patterns of the slot antenna at 8.5 GHz; substrate thickness is 1.27 mm, some substrate removed, permittivity $\epsilon_r = 10.5$, --- calculated pattern, — measured pattern. (b) *H*-plane beam patterns of the slot antenna at 8.5 GHz; substrate thickness is 1.27 mm, parts of the substrate removed, permittivity $\epsilon_r = 10.5$, --- calculated pattern, — measured pattern.

transformed by additional optics. The optimization of the antenna structure and of the effective permittivities in each section of the slotline has been done by both calculations and measurements.

B. Influence of Substrate Permittivity

It is very important to remove the dielectric substrate in the front area of the antenna, as indicated in Fig. 1, to obtain the beam patterns shown. Fig. 2 shows a pattern of an antenna with no substrate removed. This antenna receives the same power at almost all angles. In this case it is not the slotline but the dielectric material which plays the most important role. For a lower dielectric constant, for example $\epsilon_r = 2.2$ (see Fig. 4) and for a smaller substrate thickness, the beam pattern is acceptable even with no substrate removed. The shape of the antenna and the slotline parameters have not been optimized for a permittivity of $\epsilon_r = 2.2$. The intention was to make clear the influence of the different permittivities.

It is obvious that it is easier to get an acceptable performance of the antenna by using a substrate with a low permittivity or with a small thickness. To ensure that it is possible to scale the model antenna to submillimeter frequencies it is necessary to choose a material as substrate which can be fabricated with the required thickness at the final frequency. Silicon has a permittivity of 11.3, and it is

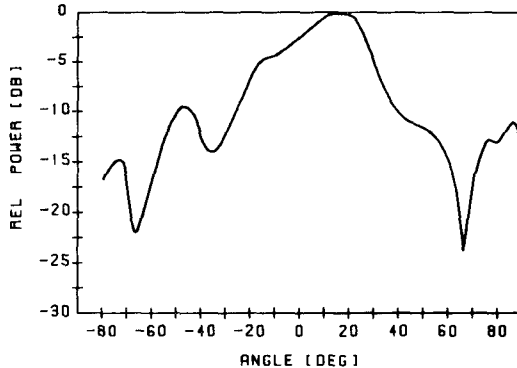


Fig. 4. *E*-plane beam pattern of the slot antenna with substrate thickness 0.63 mm; no substrate removed; $f = 8.5$ GHz, $\epsilon_r = 2.2$, measured pattern.

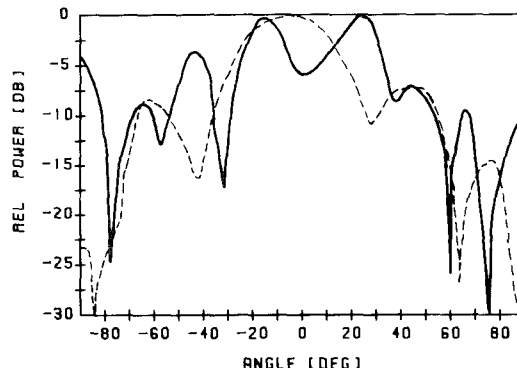


Fig. 5. Beam pattern of the slot antenna with substrate thickness 2.5 mm; parts of the substrate removed; $f = 8.5$ GHz, $\epsilon_r = 10.5$, $—$ *H*-plane pattern; $—$ *E*-plane pattern, both measured.

available with a thickness of 20 μ m. The model antenna has a substrate thickness of 1.27 mm, so that scaling to 600 GHz is possible.

In Fig. 5 the *E*- and *H*-plane beam patterns of the slot antenna on a substrate with $h = 2.5$ mm are shown. The side lobe level of the beam in the *H* plane has increased, and the beam width has become a little smaller. The beam pattern is no longer symmetric, because the *E*-plane beam has split and its side lobes are only 4 dB below maximum. This pattern cannot be regarded as an acceptable antenna pattern. A substrate thickness of 1.27 mm seems to be the upper limit at this frequency.

Most of the planar antennas that have been developed so far, for example the Vivaldi antenna [2] and other end-fire planar antennas, work with substrates and permittivities of 2 or 3 and normalized substrate thicknesses $h_n = h/\lambda_0$ lower than 0.02.

C. *E*- and *H*-Plane Beam Widths of the Antenna Patterns

The *E*- and *H*-plane beam widths depend on the length of the slot and the width of the metallized area. The 3 dB width of the *E*- and *H*-plane beams versus normalized length for two different values of the width are presented in Fig. 6. In Fig. 6(a) the width B of the antenna (see Fig. 1(b)) is 55 mm and the beam widths in the *E* and *H*

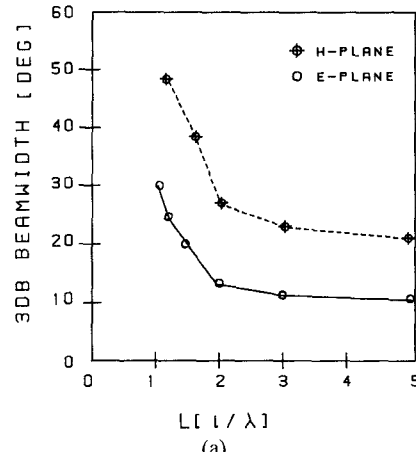


Fig. 6. (a) 3 dB beamwidth in the *E* and *H* planes versus length of the antenna, normalized to the wavelength; width B of the antenna is 55 mm.

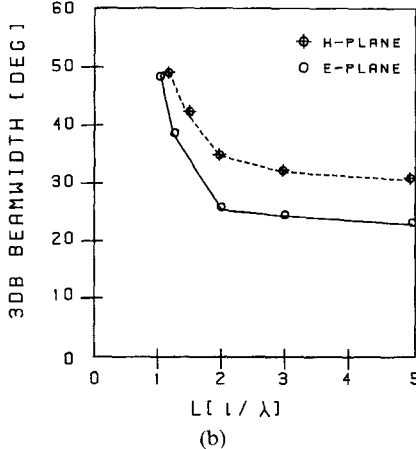


Fig. 6. (b) 3 dB beamwidth in the *E* and *H* planes versus length of the antenna, normalized to the wavelength; width B of the antenna is 75 mm.

planes are different for all normalized lengths (the slot width W_c was not changed). As expected from the theory of traveling wave antennas, the beam width decreases with increasing length of the antenna. This variation is very strong for small values of the normalized length of the antenna. The broader antenna with a width B equal to 75 mm shows a similar trend. The *H*-plane beam width has not changed very much, but the *E*-plane beam width has. For relatively short lengths, the *E*- and *H*-plane beam widths are equal. It should be noted that each point of the curves in Fig. 6 represents the optimized value of the 3 dB beam width in the *E* and *H* planes. Changing the frequency of operation or changing the length L of the slotline shows different results.

Many other parameters can be varied to improve the beam pattern, the side lobe level, and the main beam efficiency (see below). The length L_e of the exponential taper, transforming the slot impedance to 90 Ω , should be larger than the free-space wavelength. The length of the front or aperture taper L_a is less critical. The shape of the removed substrate was found to give the optimal beam pattern if it is cut along the metallization, as indicated in Fig. 1.

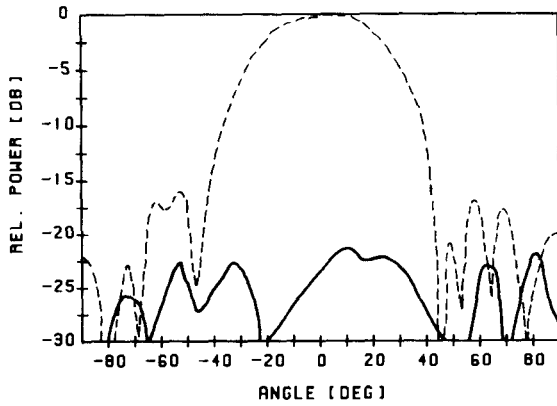


Fig. 7. Beam pattern of the slot antenna in the H plane with cross-polarization relative to the maximum of the received power in the polarized component, both measured pattern.

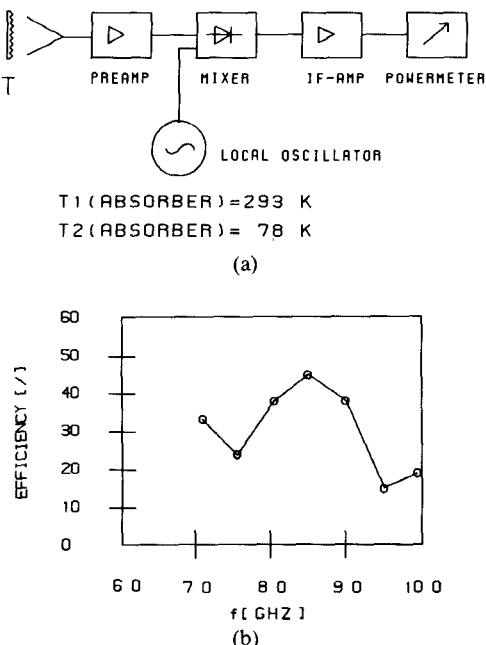


Fig. 8. (a) Equipment for measuring the main beam efficiency. (b) Main beam efficiency versus frequency.

D. Cross Polarization

The pattern described above has a maximum in the plane of the antenna (x - z plane). Measurements have been made in the E and H planes of both the polarized and cross-polarized component. The cross-polarization in the H plane is shown in Fig. 7 in dB below the maximum of the copolarized component. The cross-polarized components were measured to be more than 20 dB below maximum. In some planes the cross-polarized components are somewhat higher; in others they are lower than 20 dB below maximum.

E. Main Beam Efficiency

A complete description of the field pattern $F(\Phi, \Theta)$ requires field intensity measurements in all directions. From a complete pattern the solid angles Ω_M and $\Omega_{4\pi}$ of the main beam and of the whole pattern, respectively, can be calculated. We measured $F(\Phi, \Theta)$ at values for Φ from

-90° to 90° in steps of 5° . At each value of Φ , the pattern in the Θ direction was measured for values of Θ varying continuously from 0° to 360° . The steps between two values of Φ were 5° as a compromise between the time necessary for a complete measurement and the desired accuracy of the calculated values of the solid angles Ω_M and $\Omega_{4\pi}$. The main beam efficiency at 8.5 GHz was found to be 43 percent.

Another method was used to obtain the beam efficiency for various frequencies. The signal received by the antenna from absorbers at two different temperatures is amplified and then mixed with a tunable local oscillator signal. A power meter detects the received power (see Fig. 8(a)). The diameter of the absorber is chosen so that it fills the main beam when the absorber is in the far field. The different beam widths of the antenna patterns at different frequencies have been taken into account. To measure the main beam efficiency, the antenna is first directed to an absorber filling the whole pattern with radiation of 300 K. Then the main beam is directed to an absorber cooled by liquid nitrogen (77 K), while the stray pattern receives radiation from the warm (300 K) environment. Finally the whole pattern is directed to the cold absorber. From these three values the main beam efficiency is calculated. These measurements have been made for various frequencies by tuning the local oscillator frequency.

The measured values of the beam efficiency versus frequency are shown in Fig. 8(b). The antenna has been optimized for frequencies of 8.5 GHz. At other frequencies the main beam efficiency is lower than 45 percent. A dramatic decrease can be seen at a frequency of 9.5 GHz. From this frequency on, the side lobe level increases dramatically and the width of the main beam decreases, so that most of the power is received by the stray pattern and not by the main beam. At 8.5 GHz the values from the two methods are nearly equal.

F. Array Performance

The application of planar antennas to the construction of an array of receptors has been discussed above. It would be interesting to know whether the planar antennas can be packed closely without too much degradation of the beam patterns. The best trade-off between spacing and pattern properties has yet to be found. If the antennas are too close to each other, the beam deformation will be very strong. The main beam is no longer symmetrical, and the side lobes begin to grow. If a line of antennas is constructed, the optimal distance from a point on one slotline to the corresponding point on the next is about 20 mm (at 8.5 GHz). In this case, the beam patterns can hardly be distinguished from those of a single antenna. It has been demonstrated by Johannsson [16] that a 5×5 element array consisting of constant-width planar slot antennas works well.

III. CONCLUSIONS

A planar antenna on a dielectric substrate with a relatively high permittivity and high substrate thickness has

been developed, so that the antenna can be scaled to submillimeter wavelengths. In [1] Yngvesson *et al.* investigated various planar antennas, such as Vivaldi, LTSA, and CWSA antennas. They define an effective dielectric substrate thickness $h_{\text{eff}} = (\sqrt{\epsilon_r} - 1)h/\lambda_0$ normalized to the wavelength. Yngvesson *et al.* obtained good results with antennas on substrates with normalized thickness of 0.005 to 0.01. The technique of removing a part of the substrate allows normalized effective substrate thicknesses of 0.08. We think that this technique of removing parts of the substrate can be applied to other planar antennas as well.

The slot antenna presented here has a symmetrical beam in the *E* and *H* planes and the side lobe level is acceptable. Scaling all dimensions to submillimeter wavelengths should result in an antenna with almost the same characteristics, since the impedance Z_0 , the effective permittivity ϵ_{eff} , and the phase velocity V_{ph} depend on the normalized dimensions X_i :

$$Z_0, \epsilon_{\text{eff}}, V_{\text{ph}} = F_{z, \epsilon, v}(X_i f, X_1/X_i, X_2/X_i, \dots, \epsilon_r).$$

The functions F_z , F_ϵ , and F_v describe the dependence of the impedance Z_0 , the effective permittivity ϵ_{eff} , and the phase velocity v_{ph} on the normalized wavelength, the dimensions of the slotline, and the thickness and permittivity of the substrate.

These end-fire planar antennas can be arranged in an array so that the antennas in the same line can be placed on the same substrate. Broadside planar antennas radiate in a direction perpendicular to the plane of the antenna, so that more space is needed to integrate them into arrays. The well-known bow-tie antennas [8] and the logarithmic-periodic spiral antennas [13] are very broad band, but their beams are very broad, their beam patterns are not symmetrical, and it seems to be difficult to integrate mixer and amplifier devices because of their shape.

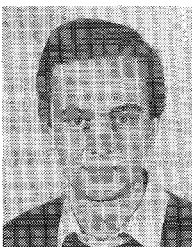
The class of end-fire planar antennas is expected to receive increased attention, especially for integrated circuit applications. Integrating some additional elements such as mixers and amplifiers in planar techniques on the same substrate makes it possible to have a "complete" receiver on a single substrate. Based on the described results we intend to scale up the model antenna to higher frequencies, to fabricate arrays of those antennas, and to integrate mixer element.

REFERENCES

- [1] K. S. Yngvesson *et al.*, "Endfire tapered slot antennas on dielectric substrates," *IEEE Trans. Antennas Propagat.*, vol. AP-33, pp. 1392-1400, Dec. 1985.
- [2] P. J. Gibson, "The Vivaldi Aerial," in *Proc. 9th Microwave Conf.* (Brighton, UK), 1979, pp. 101-105.
- [3] J. B. Knorr and K.-D. Kuchler, "Analysis of coupled slots and coplanar strips on dielectric substrates," *IEEE Trans. Microwave Theory Tech.*, vol. MTT-23, pp. 541-548, July 1975.
- [4] K. S. Yngvesson, "Near millimetre imaging with integrated planar receptors: General requirements and constraints," in *Infrared and Millimetre Waves*, vol. 10, K. Button, Ed. New York: Academic Press, 1983.
- [5] R. Janaswamy and D. H. Schaubert, "Characteristic impedance of a wide slotline on low-permittivity substrates," *IEEE Trans. Microwave Theory Tech.*, vol. MTT-34, pp. 900-902, Aug. 1986.

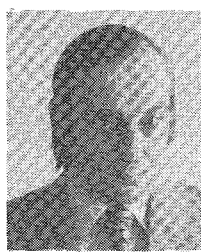
- [6] J. B. Knorr, "Slot-line transitions," *IEEE Trans. Microwave Theory Tech.*, pp. 548-554, May 1974.
- [7] K. E. Irwin, T. Van Duzer, and S. E. Schwarz, "A planar antenna-coupled superconductor-insulator-superconductor detector," *IEEE Trans. Magn.*, vol. MAG-21, pp. 216-218, Mar. 1985.
- [8] R. C. Compton, *et al.*, "Bow-tie antennas on a dielectric half space: Theory and Experiment," *IEEE Trans. Antennas Propagat.*, vol. AP-35, pp. 622-631, June 1987.
- [9] T.-L. Hwang, "Planar sandwich antennas for submillimeter application," *Appl. Phys. Lett.*, vol. 34, no. 1, pp. 9-11, Jan. 1979.
- [10] W. Hilberg, "From approximations to exact relations for characteristic impedances," *IEEE Trans. Microwave Theory Tech.*, vol. MTT-17, pp. 259-265, May 1969.
- [11] W. L. Stutzman and G. A. Thiele, *Antenna Theory and Design*. New York: Wiley, 1981.
- [12] H. J. Siweris, "Computer program description: Slot line parameters," *IEEE Trans. Microwave Theory Tech.*, vol. MTT-28, Feb. 1980.
- [13] J. D. Dyson, "The equiangular spiral antenna," *IRE Trans. Antennas Propagat.*, vol. 7, pp. 181-187, Apr. 1959.
- [14] R. Janaswamy and D. H. Schaubert, "Dispersion characteristics for wide slotlines on low-permittivity substrates," *IEEE Trans. Microwave Theory Tech.*, vol. MTT-33, pp. 723-726, Aug. 1985.
- [15] R. Janaswamy and D. H. Schaubert, "Analysis of the tapered slot antenna," *IEEE Trans. Antennas Propagat.*, vol. AP-35, pp. 1058-1065, Sept. 1987.
- [16] J. F. Johansson, "Millimetre wave imaging theory and experiments," in *Research Report No. 151*, Department of Radio and Space Science with Onsala Space Observatory, Chalmers University of Technology, Gothenberg 1986, Sweden.

✖



Ulrich Kotthaus was born in Siegen, West Germany, on July 7, 1962. He is studying physics at the University of Cologne and received the Diplom-Physiker degree in 1988.

✖



Bernd Vowinkel (M'85) received the Ing. (grad.) degree in electrical engineering from Fachhochschule Giessen, Giessen, West Germany, in 1968 and the Diplom-Physiker and Dr. degrees from the University of Bonn, Bonn, West Germany, in 1975 and 1978, respectively.

From 1968 to 1970 he was employed at a satellite tracking station operated by the European Space Agency. From 1975 to 1981 he was with the Radioastronomisches Institut of the University of Bonn, where he was concerned of low-noise millimeter-wave receiver systems. Since 1981 he has been with the 1. Physikalisches Institut of the University of Cologne, West Germany, where he is responsible for the development of millimeter- and submillimeter-wave low-noise receivers for radio astronomy and airborne radiometry.

with the development